

1 **Temperature loggers capture intraregional variation of inundation timing for**
2 **intermittent ponds**

3

4 Kerry L. Gendreau^{1†}, Valerie L. Buxton¹, Chloe E. Moore¹, Meryl C. Mims¹

5 ¹*Department of Biological Sciences, Virginia Tech, Blacksburg, VA*

6 † Email: kerryg@vt.edu

7

8

9

10 **ABSTRACT**

11 Hydroperiod, or the amount of time a lentic waterbody contains water, shapes
12 communities of aquatic organisms. Precise measurement of hydroperiod features such as
13 inundation timing and duration can help predict community dynamics and ecosystem stability. In
14 areas defined by high spatial and temporal variability, fine-scale temporal variation in inundation
15 timing and duration may drive community structure, but that variation may not be captured using
16 common approaches including remote sensing technology. Here, we provide methods to
17 accurately capture inundation timing by fitting hidden Markov models to measurements of daily
18 temperature standard deviation collected from temperature loggers. We describe a rugged
19 housing design to protect loggers from physical damage and apply our methods to a group of
20 intermittent ponds in southeastern Arizona, showing that initial pond inundation timing is highly
21 variable across a small geographic scale (~50km²). We also compare a 1-logger (pond only) and
22 2-logger (pond + control) design and show that, although a single logger may be sufficient to
23 capture inundation timing in most cases, a 2-logger design can increase confidence in results.
24 These methods are cost-effective and show promise in capturing variation in intraregional
25 inundation timing that may have profound effects on aquatic communities, with implications for
26 how these communities may respond to hydroperiod alteration from a changing climate.

27 **Key Words: temporary ponds, hydroperiod, HOBO Pendant logger, temperature sensor,**
28 **hidden Markov models, American Southwest, aquatic, desert**

29
30
31
32
33
34
35
36

37 **1. Introduction**

38 For water-dependent organisms, hydroperiod – or the amount of time a lentic waterbody holds
39 water – plays a critical role in population and community dynamics (De Meester et al., 2005).
40 Dispersal decisions (Tournier et al., 2017), fitness (Johnson et al., 2013; Rogers & Chalcraft,
41 2008), reproductive success (Ryan & Winne, 2001), survival (Acosta & Perry, 2001), and
42 source-sink dynamics (Ruetz III et al., 2005; Werner et al., 2007) are all influenced by
43 hydroperiod. Hydroperiod is also an important predictor of community composition (Razgour et
44 al., 2010; Skelly, 1997; Waterkeyn et al., 2008) and diversity (Schriever et al., 2015; Schriever &
45 Williams, 2013; Stendera et al., 2012), and thus may influence ecosystem stability. Specific
46 components of hydroperiod, such as inundation timing or stability, influence species density and
47 richness (Florencio et al., 2020; Kneitel, 2014) may play a key role in determining reproductive
48 success of amphibians (Paton & Crouch III, 2002).

49 The wide-ranging effects of hydroperiod on individual organisms, populations, and
50 ecological communities necessitate tools to enable fine-scale measurement and monitoring of the
51 timing, frequency, and duration of hydroperiod events in temporary lentic waters. Such tools will
52 play an important role in predicting how hydroperiods may change in response to future water
53 use and climate scenarios – and how organisms that rely on these habitats will fare. Satellite
54 remote sensing tools such as Synthetic Aperture Radar (Bourgeau-Chavez et al., 2005; Hong et
55 al., 2010) and Landsat imagery (DeVries et al., 2017; Díaz-Delgado et al., 2016; Murray-Hudson
56 et al., 2015) enable wetland hydroperiod assessment over multi-year or multi-decade periods and
57 covering 10s to 1000s km². The accuracy of these methods continues to improve with advances
58 in image analytical techniques that provide information on surface water presence and area at a
59 sub-pixel level (Halabisky et al., 2018). Despite these promising advances, the temporal grain of

60 remotely sensed data remains coarse for most remotely sensed datasets. For example, Landsat
61 captures images at a spatial resolution of 30 meters every 16 days (Irons et al., 2012; Ozesmi &
62 Bauer, 2002). Remotely-sensed images can be obscured by cloud cover, further decreasing
63 temporal resolution. In many regions, inundation of intermittent lentic habitat may occur over
64 hours or days. Temporal resolution on the order of 2-4 weeks may miss important fine-scale
65 differences in pond inundation timing, particularly in regions with unpredictable spatial patterns
66 of precipitation that drive a patchwork of inundation dates.

67 Temperature and conductivity sensors are used increasingly in both lotic and lentic
68 systems to provide fine-scale spatial and temporal hydroperiod measurements (Anderson et al.,
69 2015; Arismendi et al., 2017; Jaeger & Olden, 2012). Daily temperature variance is typically
70 lower in water than in air, and comparison of daily temperature variance provides a reliable
71 proxy for inundation state (Sowder & Steel, 2012). A rapid drop in daily temperature variance
72 can reliably measure the precise timing of an inundation event (Anderson et al., 2015; Arismendi
73 et al., 2017). For example, Anderson et al. (2015) tested the ability of temperature sensors to
74 accurately predict inundation states both in natural wetlands and in controlled mesocosms. The
75 authors deployed temperature sensors for two six-month periods in ponds over a 7140 ha area
76 that varied in size and depth. They demonstrated that daily temperature variance reflected pond
77 filling and drying events, with higher variance in dry ponds and in control sensors placed on the
78 ground outside of ponds, and they determined an approximate variance threshold to predict
79 inundation states. Arismendi et al. (2017) placed paired temperature sensors and electrical
80 resistors in temporary streams. They found that using daily temperature standard deviation more
81 accurately predicted inundation states than mean hourly or daily temperature measurements, and
82 they applied 2-state hidden Markov models, which account for autocorrelation of time series

83 data, to the daily temperature standard deviations measured from the streams in order to predict
84 shifts from wet to dry states.

85 Here, we describe methods for deployment and data analysis of an array of temperature
86 loggers to monitor inundation state of intermittent ponds in the San Rafael Valley of Arizona,
87 USA. The objectives of this study were: 1) design a sturdy, low cost, and low maintenance
88 housing unit for temperature sensor deployment in remote and rugged terrain; 2) deploy paired
89 sensors (one within the target pond and one outside the pond) to monitor hydroperiod inundation
90 states in temporary ponds; 3) evaluate inundation states using hidden Markov models, comparing
91 inundation date inference between 1-logger (pond only) and 2-logger (pond + control)
92 experimental design; 4) compare observed and inferred inundation state recorded during in-
93 person visits to ponds. Overall, our findings point to the utility of temperature loggers as a cost-
94 effective, low profile tool in uncovering ecologically relevant spatiotemporal differences in
95 intraregional inundation timing. This is particularly useful in regions with highly localized
96 precipitation events that drive small-scale differences in spatiotemporal hydroperiod dynamics.

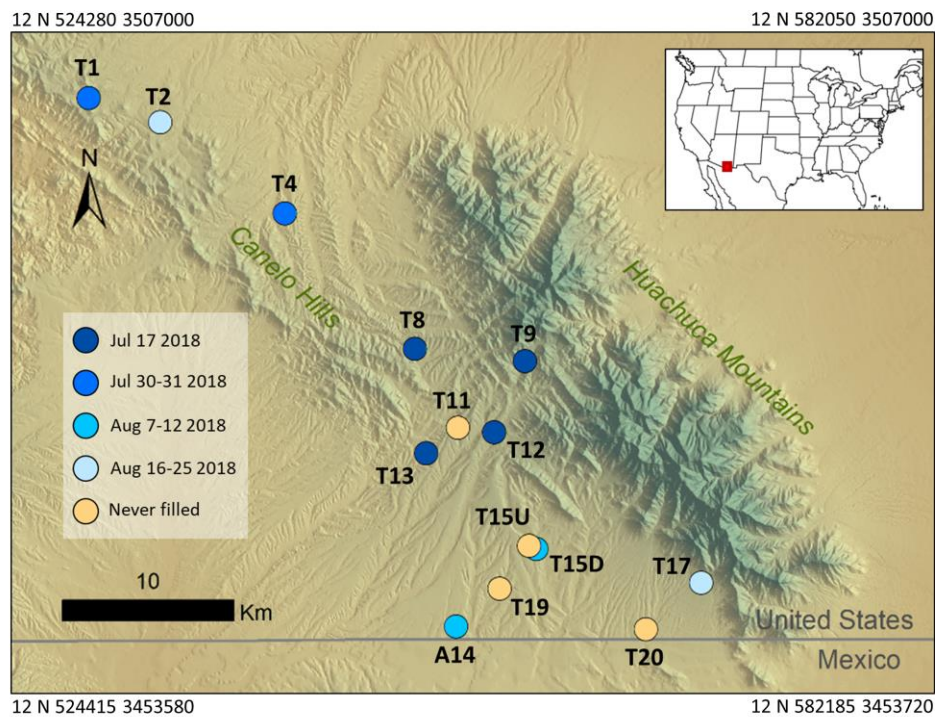
97

98 **2. Methods**

99 **2.1 Study area**

100 We deployed paired temperature loggers (one within and one outside a pond) in 16 intermittent
101 ponds in the Coronado National Forest, located within the Huachuca Mountains Canelo Hills
102 (HMCH) region and San Rafael Valley of southeastern Arizona, USA in June and July 2018
103 (Figure 1). The HMCH region is part of the Madrean Sky Islands, with an elevation range of
104 approximately 1150 m to 2880 m. Habitat composition includes cienega wetlands, semi-arid
105 grasslands and thorn-scrub, and evergreen and coniferous woodlands. The climate of this region

106 is semi-arid, with up to half of the annual rainfall occurring during the summer monsoon season
 107 (Sheppard et al., 2002). Rain events during the monsoon season are typically short in duration,
 108 high in intensity, and seasonally predictable but spatially variable (Goodrich et al., 2008). Ponds
 109 in the region were originally constructed to provide water for livestock and are often called
 110 “stock tanks”; these ponds are now surrogating for aquatic habitat lost to human activities and
 111 support a range of aquatic species (Rosen & Schwalbe 1998; Storfer et al. 2014; Mims et al.
 112 2016). We selected ponds based on historical hydroperiod data that indicated they were generally
 113 intermittent and tended to have longer (>1 month) duration wetted phases (Parsley et al., 2020).



114 **Figure 1.** Study ponds (N=14) in the Huachuca Mountains-Canelo Hills region of southeastern
 115 Arizona (reference map inset). Colors indicate pond initial fill dates, ranging from 17 July 2018
 116 (T8, 9, 12, and 13) to 25 August 2018 (T2). Initial fill dates were calculated from paired pond-
 117 control Hidden Markov models, where inundation was defined as a period of 5 or more
 118 consecutive days with the daily temperature standard deviation measured by the pond logger was
 119 at least 2°C less than that of the control logger. UTM coordinates (NAD 83) indicate position of
 120 each corner of the map.

121

122

123 **2.2 Sensors, housing units, and deployment**

124 We selected a waterproof temperature logger with the capacity for battery replacement by the
125 user for longevity (company: Onset, Bourne, MA, USA; model: HOBO Pendant, MX2201;
126 diameter: 3.35 cm; temperature range: -20 °C to 50°C; temperature precision: $\pm 0.5^\circ\text{C}$; cost:
127 \$54.00 USD; data retrieval: Bluetooth, battery: user replaceable CR2032 3V lithium). Our study
128 region is remote with rugged terrain, and deployed equipment is exposed to variable weather,
129 UV exposure, and potential tampering from humans, wildlife, or livestock. The intermittent
130 ponds in our study region are visited frequently by cattle, and equipment must be able to
131 withstand trampling or tampering. With this in mind, we designed a rugged housing unit to
132 protect temperature loggers from damage and ensure long-term durability (Figure S1). We
133 placed a logger inside a PVC junction box (hereafter called the housing unit) with two nuts
134 between the box and the lid for increased air or water flow. The logger moved freely inside the
135 housing unit to increase the chance that it remained submerged (i.e., fell to the lowest point
136 within the housing unit) if disturbed after deployment. The housing unit was connected to a
137 concrete tie or other secure post (e.g., a metal fence post marking edges of allotments) via a
138 3/32" (2.381 mm) galvanized, uncoated steel cable strung through the holes of the junction box.
139 We fastened the cable by swaging a crimping sleeve. We provide a complete list of
140 specifications for tools and materials in Table S1.

141 At each of the 16 ponds, we deployed one logger at the approximate deepest point of fill
142 within the tank (the pond logger) and one logger approximately 10 m outside of the high-water
143 mark for the pond (the control logger). Where possible, we placed control loggers in sunny,

144 shade-free areas in order to most closely match conditions and exposure of the pond logger. If
145 the pond basin consisted of fine clay or silt, we placed the housing unit on a flat rock partially
146 buried to sit flush with the ground and to avoid it becoming buried in silt upon pond inundation.
147 We then secured the housing unit to an existing fence post (typically a metal T post) or to a
148 concrete tie using steel cable looped through the housing. We used a mallet to drive concrete ties
149 completely into the ground for protection of livestock. Finally, we covered units with loosely
150 stacked rocks to minimize livestock tripping risk and to help camouflage units to avoid
151 tampering (Figure S2). Loggers recorded temperature at 15-minute intervals with Bluetooth set
152 to manual (i.e., not continuously seeking a signal), resulting in an estimated 3.2-year battery life
153 for each logger. We visited ponds three times after sensor deployment: 31 Jul – 2 Aug 2018, 31
154 Mar - 3 April 2019, and 21 – 27 June 2019 (time of data retrieval).

155

156 **2.3 Prediction of pond inundation states using Hidden Markov models**

157 We used a custom script in R v3.6.1 (R Development Core Team, 2018) to calculate the daily
158 temperature standard deviations (tSDs) measured by each temperature logger. We then used the
159 package depmixS4 v1.4.0 (Visser & Speekenbrink, 2010) in R to fit hidden Markov models
160 (HMMs) to detect temporal shifts in tSD, representing pond filling and drying events. HMMs
161 can be used to identify shifting trends in time series data (e.g. high tSDs associated with dry
162 states and low tSDs associated with wet states) while accounting for temporal autocorrelation.
163 Therefore, they are useful tools for modeling climatic data (reviewed in Srikanthan & McMahon,
164 2001). We initially fit both 2-state and 3-state HMMs to both of our datasets, with the former
165 modeling a simple scenario of distinct dry and wet states, and the latter factoring in the potential
166 effects of seasonal differences, which may cause daily tSD readings to differ due to varying

167 water depths above the sensors (Anderson et al., 2015) or as a result of seasonal environmental
168 variation (Campbell & Diebold, 2005). We compared two different datasets for each study site:
169 one using temperature data from the paired pond and control loggers at each site, calculated by
170 subtracting the tSDs of the pond loggers from the tSDs of control loggers (wherein a value of 0
171 indicates no difference in daily tSD between the pond and air temperatures), and another using
172 tSDs from pond loggers only.

173

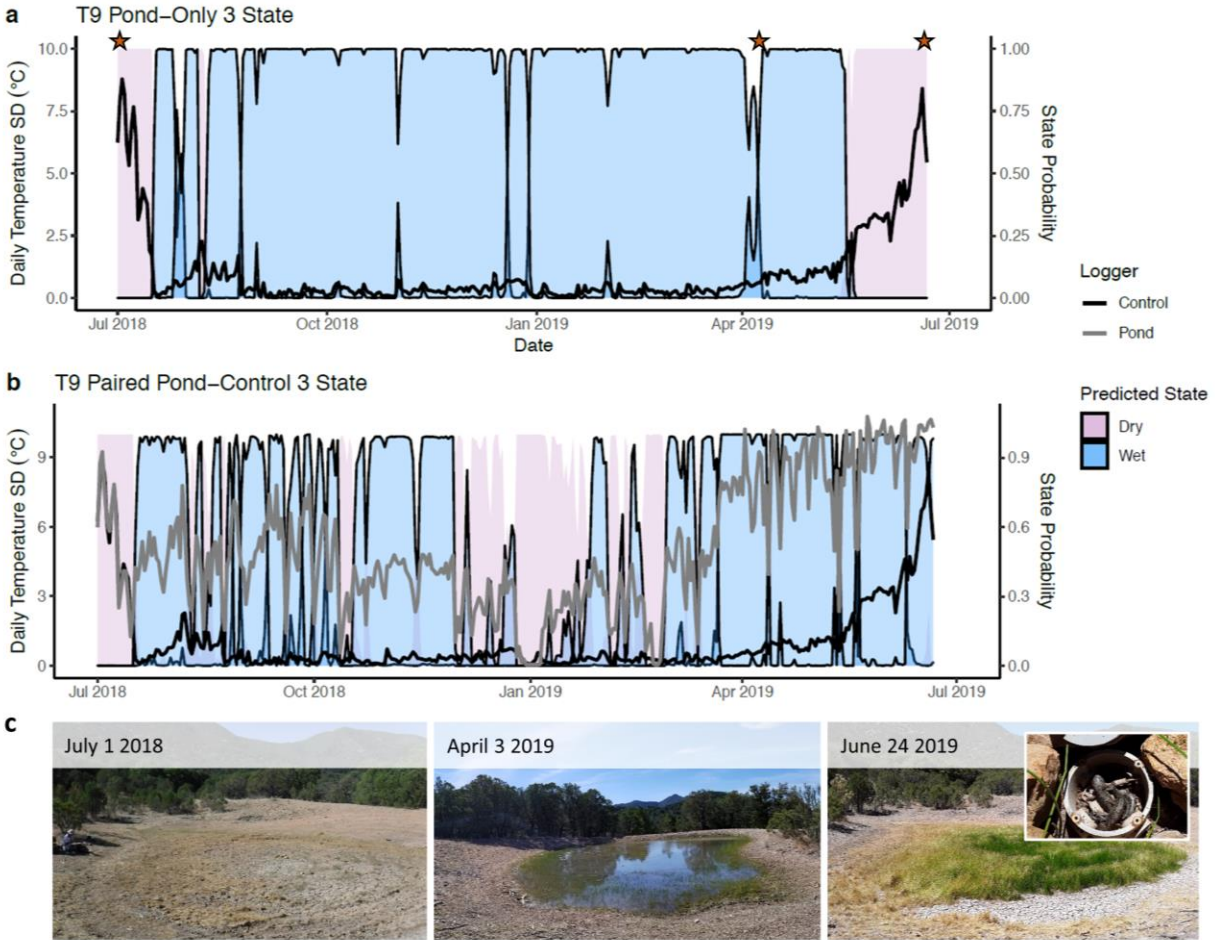
174 **3. Results and Discussion**

175 **3.1 Assessment of housing unit performance**

176 We retrieved data from 30 (n = 14 pond loggers, n = 16 control loggers) of the 32 loggers
177 deployed, with two pond loggers underwater at the time of collection. We downloaded
178 temperature data for the entire study period (between 1 July 2018 and 21 June 2019) for 26
179 loggers. Four pond loggers at sites T1, T2, T8, and T13 failed due to a potentially faulty logger
180 backing design that was addressed by the manufacturer during the time between initial
181 deployment and site visits in June 2019; all pond loggers were replaced by the manufacturer, and
182 replacements were deployed following data retrieval in June 2019. No subsequent issues
183 emerged (0% failures) using loggers with the updated backing for other experiments during
184 which loggers were submerged in water for months at a time (M.C. Mims, unpublished data).
185 During each site visit, we evaluated logger function, cleared any mud or sediment in the rugged
186 housing units, and replaced disturbed rock piles (Figure S3).

187 Overall, we found that the logger design accomplished our goals, but there were some
188 considerations and limitations. Our logger housing design successfully protected the loggers
189 from physical damage, even when disturbed by cattle. Careful placement of loggers in the

190 deepest point in the pond is also imperative for accurate hydroperiod estimation. At site T11, we
191 observed that the pond logger did not appear to be placed at the lowest point within the pond, as
192 was intended. We observed very shallow water pooled in another location near the logger in
193 summer 2019 that dried a few days later. Therefore, the data collected from this logger may not
194 accurately reflect the pond inundation state. The other issue with our physical design was the
195 accumulation of sediment or other debris within the rugged housing unit that contain the logger
196 and interfered with temperature readings from the pond loggers at sites A14, T4, T9, and T17
197 (see Figure S3 for example). We occasionally observed animals inside housing units, including
198 several salamanders inside the housing for the pond logger at site T9 (Figure 2). Additionally,
199 rock piles placed on top of the rugged housing likely affected absolute temperature readings.
200 Though rock color or density may have had differential effects among loggers, we suspect the
201 variation among loggers was likely low overall. Furthermore, because this method considers tSD
202 rather than absolute temperature, we do not anticipate these differences had substantial effects on
203 results.



204 **Figure 2.** Three-state hidden Markov model predictions for pond T9 using (a) pond-only dataset,
 205 and (b) paired pond-control dataset. (c) Photos from site visits (dates correspond with stars in
 206 (a)), in which observed pond inundation state was dry at the time of sensor deployment (1 July
 207 2018), wet during a return visit the following spring (3 April 2019), and dry at the time of sensor
 208 retrieval (24 June 2019). Though we observed no standing water on 24 June 2019, the pond
 209 supported vegetation, and we found salamanders in the sensor housing unit (inset photo; possibly
 210 contributing to different predicted states on 24 June 2019). Colors indicate temporal state
 211 predictions for each pond (pink=dry, blue=wet) and lines represent daily temperature standard
 212 deviation (tSD) measurements from pond logger (black lines) and control logger (grey lines).

213

214

215

216

217 **3.2 Comparison of 2- versus 3-state Hidden Markov models and determination of wet state**
218 **threshold values**

219 Because the fit() function in depmixS4 will force each dataset into the designated number of
220 states, even in the absence of a true wet state, we used the HMM parameter estimates to
221 determine appropriate tSD thresholds to designate each state as “wet” or “dry” for both datasets,
222 comparing the predicted states to the known states of the ponds during our four site visits (Tables
223 S2 and S3). For the paired pond-control dataset, we used a wet state threshold of -2.0°C ,
224 meaning that the daily tSDs measured by the pond sensors were at least 2.0°C lower on average
225 than those measured by the control sensors. This -2.0°C threshold minimized the number of false
226 dry state predictions. It did result in a false wet prediction for T17, but this was likely due to
227 sediment in the pond sensor housing that may have affected the reading. A more conservative
228 threshold of -2.2°C falsely predicted T12 as dry (Table S3).

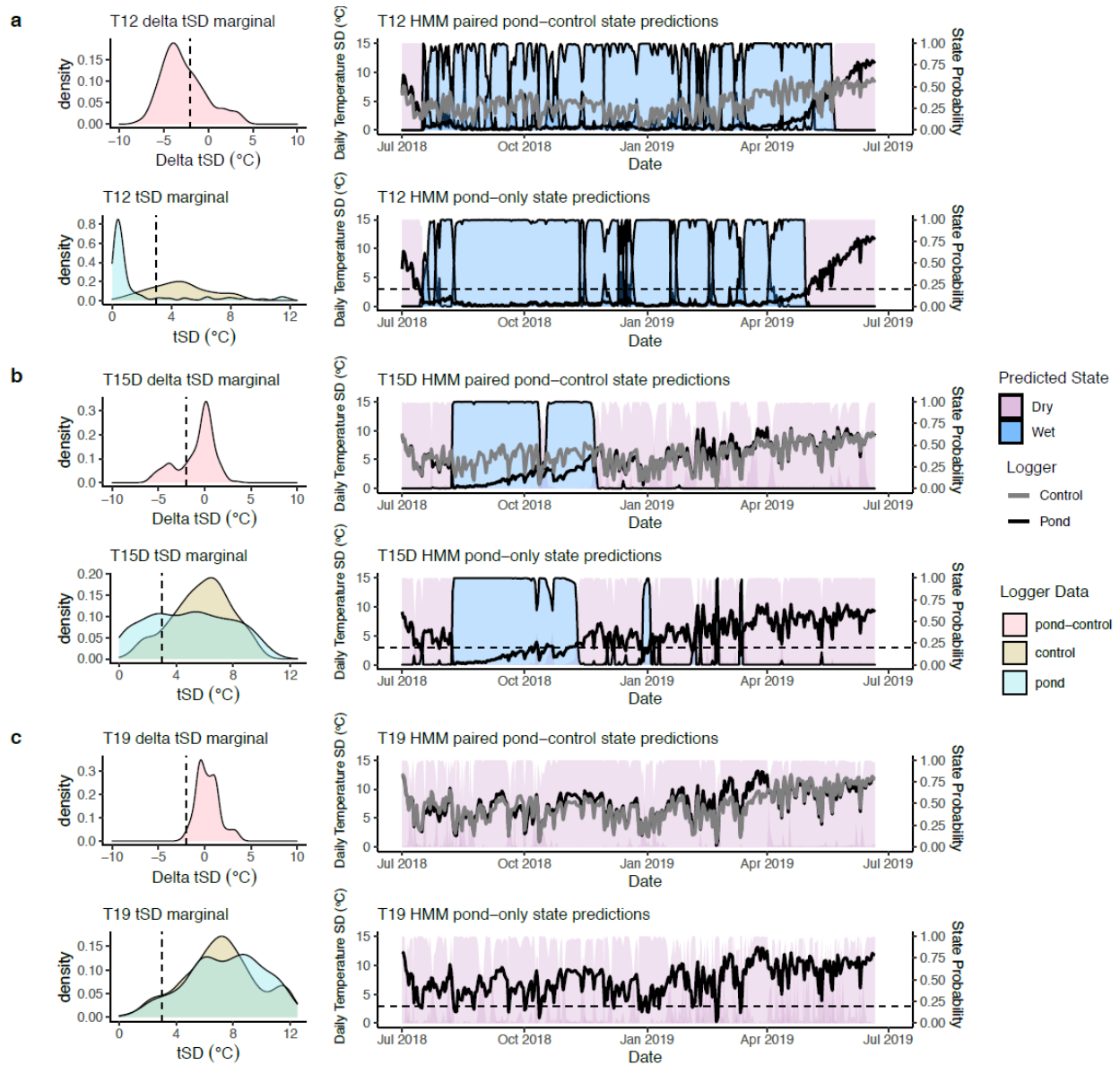
229 Use of HMMs with >2 states can help resolve variation among dry-wet states, improving
230 classifications. Although 2-state HMMs have been applied in past work (Arismendi et al., 2017),
231 we found that 2-state HMMs appeared to over- or underestimate inundation duration for several
232 ponds or predict additional wet states when we were confident that the ponds were dry (Figure
233 S4). Using 3-state HMMs and subsequently combining multiple wet or dry states provided more
234 accurate and consistent state predictions between pond only and paired pond-control datasets
235 (Tables S2, S3). Anderson et al. (2015) showed that seasonal fluctuation, canopy cover, pond
236 vegetation, and water depth can influence temperature variance readings from temperature
237 loggers placed in wetland basins, and that loggers in relatively deeper water have lower variance
238 than those in shallower water. Therefore, we focused our analyses on results from the 3-state
239 HMMs, which allow for the potential for seasonal variation in daily tSDs and intermittent wet-

240 dry states (e.g., damp), accounting for potential uncertainty due to wet sediment or other factors
241 (see Figure 3 for examples).

242 Upon fitting 3-state HMMs to the pond-only dataset, we found that a threshold between
243 2.9°C to 3.3°C minimized the number of false dry states for most ponds (Table S2, Table S3).
244 This threshold is slightly lower than that proposed by Anderson et al. (2015), who determined
245 that using daily temperature variances cutoffs between 13 and 15 (corresponding to tSDs
246 between 3.6°C and 3.9°C) for the wet state provided the most accurate predictions of pond
247 inundation states in their field experiments. Within our pond-only dataset, using a less
248 conservative tSD threshold of 3.5°C decreased the accuracy leading to a false wet state
249 prediction for pond T15U. For pond T8, the state with the highest average temperature standard
250 deviation (~2.8°C) fell below our wet state cutoff of 3.0°C (Table S5). Because we knew that the
251 pond was dry at two timepoints in this state (during logger deployment and logger retrieval), we
252 decreased the wet state threshold to 2.7°C for this particular pond and considered the average
253 tSD of 2.8°C to reflect a dry state.

254 To further define a “reliable” wet state prediction from our HMMs, we also required that
255 the pond remain in a given state for a minimum of 5 consecutive days. We chose this cutoff
256 based on site observations in early August 2018, during which ponds T17 and T20, which had
257 short predicted wet states of 7 and 5 days in July respectively, both showed evidence of prior
258 inundation despite being dry at the time of our visit, and pond A14, which had a predicted wet
259 state of 4 days in mid-July but showed no evidence of earlier inundation in early August (Table
260 S2, Table S3).

261



262 **Figure 3.** Inundation state predictions by 3-state hidden Markov models (HMMs). Shown are
 263 marginal distributions and predicted inundation timing for select ponds that (a) became
 264 inundated for long durations during the study period, (b) filled for relatively shorter durations,
 265 and (c) had no predicted wet state. Left panels represent marginal distributions and right panels
 266 represent HMM estimates from paired pond-control models (top) and pond-only models
 267 (bottom). Shading on HMM graphs indicate temporal state predictions for each pond (pink=dry,
 268 blue=wet) and lines represent temperature standard deviation (tSD) measurements from control
 269 loggers (grey lines) and pond loggers (black lines). Dashed lines indicate wet state thresholds
 270 (3.0°C for the pond only dataset and -2.0°C difference for the paired dataset).
 271

272

273 3.3 Pond inundation regimes

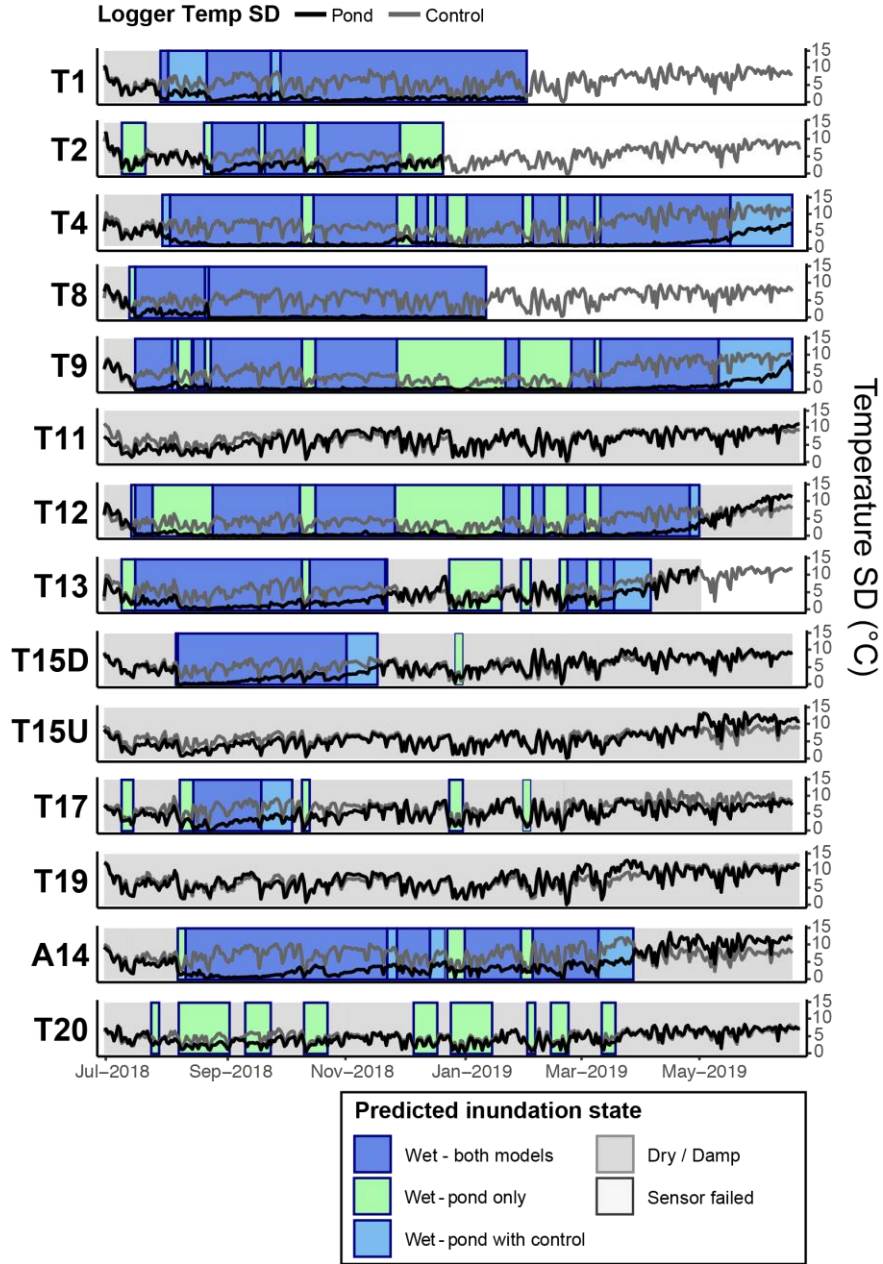
274 Under the wet state criteria defined above, 3-state HMMs for the pond-only model accurately
275 predicted inundation states for 92% of site visits for the 14 ponds. The paired pond-control
276 model accurately predicted inundation states for 90% of sites visits. Most of the incorrect state
277 predictions were likely due to sediment or additional debris accumulating within the rugged
278 housing units, which was more likely to affect precision of drying dates rather than initial
279 inundation timing.

280 Based on HMM estimates, ponds varied in both initial timing and duration of inundation
281 (Figure 4), with initial inundation dates ranging from 10 July 2018 to 7 August 2018, over a
282 small geographic area (Figure 1). Eleven of the fourteen ponds in our study had at least one
283 predicted wet state during our monitoring period. Ten of these ponds had wet states predicted
284 from both datasets. Based on the state predictions by both models, ponds in the central range of
285 our study area filled first, with ponds T8, T9, T12, and T13 all inundated between 10 - 17 July
286 2018. Ponds in the northern and southern portions of the study area had more variation in their
287 initial inundation dates, which were predicted to occur between late July and mid-August (Table
288 S6, Figure 1, Figure 4).

289 Disagreement between pond-only and pond-control models regarding whether or not a pond
290 filled was rare. Only pond T20 was predicted to have a wet state by one model (the pond-only
291 model) and not the other. The presence of vegetation at the perimeter of the pond and mud inside
292 the housing of the T20 pond logger during our visit in April 2019 suggest that the pond may have
293 been inundated with water at some point during logger deployment. Visual inspection of the T20
294 temperature standard deviation readings revealed a slight difference between August and
295 October 2018. Ponds T11 and T15U, which had no predicted inundation dates, also showed

296 slightly lower readings from the pond loggers relative to the control loggers at certain points in
297 the monsoon season and had mean state values close to but slightly above our wet state
298 thresholds. It is possible that some water accumulated in these ponds and that our wet state
299 threshold for the HMMs lacked the sensitivity to capture these low signals. The tSD threshold
300 may need to be adjusted to increase precision in cases where small amounts of water accumulate
301 for durations shorter than 5 days.

302



304 **Figure 4.** Hidden Markov model (HMM) pond inundation predictions. Lines show daily tSDs
 305 measured by pond loggers (black) and control loggers (grey). Rectangles represent wet days
 306 predicted by HMMs from single pond loggers (light green), by paired pond-control loggers (light
 307 blue), and by both models (dark blue). Grey shading indicates a predicted dry/damp state and
 308 lack of shading indicates no data due to logger failure.
 309

311 **3.4 Comparison of 1 (pond-only) versus 2 (paired pond-control) logger design**

312 Models using temperature data from pond loggers alone predict inundation states that closely
313 aligned with those using paired pond-control logger data, indicating that a single logger design
314 may be sufficient to capture inundation timing of longer-duration events (Table S5, Figure 4).
315 However, control logger data may help alleviate some of the wet state false-positives,
316 particularly when the standard deviation of daily air temperature is relatively low or issues such
317 as sediment in rugged housing units occur. For example, earlier inundation dates are predicted
318 for several ponds by the pond-only model relative to the paired pond-control model. This may be
319 a true wet state, or the coincident low temperature standard deviations measured by the control
320 loggers may have simply resulted in lower variance in the temperature on those days. For site
321 T13, the state was correctly predicted as wet by the paired pond-control model, but not by the
322 pond-only model in April 2019. While we did observe water in the pond at this time, the water
323 level was just at the base of the rock pile covering the logger housing, which may explain the
324 discrepancies between the models. In cases such as this when shallow water is present, the 2-
325 logger design may help to increase the probability of detecting inundation. Predicting pond
326 drying may require an array of pond loggers situated at different heights within in the pond to
327 capture this fine-scale variation. But considerations exist for the pond-control logger model as
328 well. For example, pond-only models predicted wet states for most ponds in the winter months
329 (between December and February) that were not predicted by the paired pond-control models.
330 The relatively low tSDs of the loggers in the winter months may be due to snow accumulation on
331 top of the control loggers.

332 Although we have relatively high confidence in inundation timing, drying dates were less
333 precise largely due to the accumulation of sediment in the housing unit. Paired pond-control

334 models also predicted later drying states for ponds T4, T9, and A14. At site A14, mud was
335 discovered in the logger housing on 31 March 2019 and was cleared. In the days preceding 31
336 March 2019, the temperature standard deviations from the pond logger were considerably lower
337 than those from the control logger at this site, despite a lack of water in the pond, resulting in the
338 paired pond-control model falsely predicting that the pond was in a wet state. After the sediment
339 was cleared, the difference in these tSDs decreased to nearly zero, and the paired pond-control
340 model correctly designated the pond state as dry. Mud and debris found inside the rugged
341 housing of the pond loggers at sites T4 and T9 in late June likely caused the tSDs of these pond
342 loggers to remain low relative to those of the control loggers even after drying, leading to false
343 wet predictions.

344 To improve drying date precision, the housing unit design would likely need to exclude
345 sediment, which is difficult to do without making other compromises. Solutions for avoiding the
346 issue of sediment packing in rugged housing units, and the subsequent decoupling of pond and
347 control data, include packing the housing unit with insulation or other material that would not
348 allow sediment to enter. However, this can lead to issues such as a buoyant housing unit and may
349 affect the temperature readings if the material is a good insulator. Conductivity sensors offer an
350 alternative to temperature loggers. However, custom modifications required to create
351 conductivity sensors can be time-consuming or, if outsourced, may result in units that are >2
352 times the cost of temperature loggers. Additionally, conductivity sensors may suffer from the
353 same issues related to poor or imprecise detection of drying patterns due to water trapped in
354 sediments. Temperature measurements offer data that are biologically meaningful (temperature
355 as well as presence/absence of water) and that may address multiple needs depending on the
356 objectives of a study.

357
358
359
360
361
362
363
364
365
366
367
368
369
370

4. Conclusions

Precise measurement of pond inundation timing can be essential for studies of ecological and hydrological dynamics, particularly in areas with fine-scale variation in climate, where limited water supply may be crucial in shaping population and community dynamics. In this study, we observed an approximate 4-week difference in initial inundation timing between ponds within a small geographic range (~50km²), which is a substantial portion of the aquatic stage for many aquatic organisms that rely on these ponds to complete their life cycle (e.g., amphibians: Mims et al., 2020; Moore et al., 2020); these intraseasonal differences in inundation timing may thus have major implications for community composition and species turnover in these habitats. Fine-scale hydrological data such as those presented herein provide valuable information about dynamic water regimes that can improve conservation strategies by identifying potential refugees for plants and wildlife and can also aid in planning for human adaptation in response to the changing climate.

371

Acknowledgments, Samples, and Data. J. Kraft, M.J. Farruggia, J.A. Smith, S.A. Yamada, and J.C. Uyeda and the Uyeda Lab provided input and feedback on experimental design and data analysis. M.A. Hallmark, J. Kraft, M.B. Parsley, and E.J. Shadle helped with sensor deployment and data collection in the field. All fieldwork was done with permission from the Coronado Ranger District of the U.S. Forest Service. Funding for this work was provided by the College of Science and Fralin Life Sciences Institute at Virginia Tech and by a graduate fellowship to KLG from the Interfaces of Global Change program at Virginia Tech. Data, supplementary materials, and R code associated with this manuscript will be linked to Zenodo prior to publication, and are currently available at: (<https://github.com/MimsLabVT/PondsProject>).

381
382
383
384
385
386

387 **References**

- 388 Acosta, C. A., & Perry, S. A. (2001). Impact of hydroperiod disturbance on crayfish population
389 dynamics in the seasonal wetlands of Everglades National Park, USA. *Aquatic*
390 *Conservation: Marine and Freshwater Ecosystems*, 11(1), 45-57.
391 <https://doi.org/10.1002/aqc.426>
- 392 Anderson, T. L., Heemeyer, J. L., Peterman, W. E., Everson, M. J., Ousterhout, B. H., Drake, D.
393 L., & Semlitsch, R. D. (2015). Automated analysis of temperature variance to determine
394 inundation state of wetlands. *Wetlands Ecology and Management*, 23(6), 1039-1047.
395 <https://doi.org/10.1007/s11273-015-9439-x>
- 396 Arismendi, I., Dunham, J. B., Heck, M., Schultz, L., & Hockman-Wert, D. (2017). A statistical
397 method to predict flow permanence in dryland streams from time series of stream
398 temperature. *Water*, 9(12), 1-13. <https://doi.org/10.3390/w9120946>
- 399 Bourgeau-Chavez, L. L., Smith, K. B., Brunzell, S. M., Kasischke, E. S., Romanowicz, E. A., &
400 Richardson, C. J. (2005). Remote monitoring of regional inundation patterns and
401 hydroperiod in the Greater Everglades using Synthetic Aperture Radar. *Wetlands*,
402 25(176). [https://doi.org/10.1672/0277-5212\(2005\)025\[0176:RMORIP\]2.0.CO;2](https://doi.org/10.1672/0277-5212(2005)025[0176:RMORIP]2.0.CO;2)
- 403 Campbell, S. D., & Diebold, F. X. (2005). Weather forecasting for weather derivatives. *Journal*
404 *of the American Statistical Association*, 100(469), 6-16.
405 <https://doi.org/10.1198/016214504000001051>
- 406 De Meester, L., Declerck, S., Stoks, R., Louette, G., Van De Meutter, F., De Bie, T., et al.
407 (2005). Ponds and pools as model systems in conservation biology, ecology and
408 evolutionary biology. *Aquatic Conservation: Marine and Freshwater Ecosystems*, 15(6),
409 715-725. <https://doi.org/10.1002/aqc.748>
- 410 DeVries, B., Huang, C., Lang, M. W., Jones, J. W., Huang, W., Creed, I. F., & Carroll, M. L.
411 (2017). Automated quantification of surface water inundation in wetlands using optical
412 satellite imagery. *Remote Sensing*, 9(8), 807. <https://doi.org/10.3390/rs9080807>
- 413 Díaz-Delgado, R., Aragonés, D., Afán, I., & Bustamante, J. (2016). Long-term monitoring of the
414 flooding regime and hydroperiod of Doñana marshes with Landsat time series (1974–
415 2014). *Remote Sensing*, 8(9), 775. <https://doi.org/10.3390/rs8090775>
- 416 Florencio, M., Fernández-Zamudio, R., Lozano, M., & Díaz-Paniagua, C. (2020). Interannual
417 variation in filling season affects zooplankton diversity in Mediterranean temporary
418 ponds. *Hydrobiologia*, 847, 1195-1205. <https://doi.org/10.1007/s10750-019-04163-3>
- 419 Goodrich, D. C., Unkrich, C. L., Keefer, T. O., Nichols, M. H., Stone, J. J., Levick, L. R., &
420 Scott, R. L. (2008). Event to multidecadal persistence in rainfall and runoff in southeast
421 Arizona. *Water Resources Research*, 44(5). <https://doi.org/10.1029/2007wr006222>
- 422 Halabisky, M., Babcock, C., & Moskal, L. M. (2018). Harnessing the temporal dimension to
423 improve object-based image analysis classification of wetlands. *Remote Sensing*, 10(9),
424 1467. <https://doi.org/10.3390/rs10091467>
- 425 Hong, S.-H., Wdowinski, S., Kim, S.-W., & Won, J.-S. (2010). Multi-temporal monitoring of
426 wetland water levels in the Florida Everglades using interferometric synthetic aperture
427 radar (InSAR). *Remote Sensing of Environment*, 114(11), 2436-2447.
428 <https://doi.org/10.1016/j.rse.2010.05.019>
- 429 Irons, J. R., Dwyer, J. L., & Barsi, J. A. (2012). The next Landsat satellite: the Landsat data
430 continuity mission. *Remote Sensing of Environment*, 122, 11-21.
431 <https://doi.org/10.1016/j.rse.2011.08.026>

432 Jaeger, K. L., & Olden, J. D. (2012). Electrical resistance sensor arrays as a means to quantify
433 longitudinal connectivity of rivers. *River Research and Applications*, 28(10), 1843-1852.
434 <https://doi.org/10.1002/rra.1554>

435 Johnson, J. R., Ryan, M. E., Micheletti, S. J., & Shaffer, H. B. (2013). Short pond hydroperiod
436 decreases fitness of nonnative hybrid salamanders in California. *Animal Conservation*,
437 16(5), 556-565. <https://doi.org/10.1111/acv.12029>

438 Kneitel, J. M. (2014). Inundation timing, more than duration, affects the community structure of
439 California vernal pool mesocosms. *Hydrobiologia*, 732(1), 71-83.
440 <https://doi.org/10.1007/s10750-014-1845-1>

441 Mims, M. C., Moore, C. E., & Shadle, E. J. (2020). Threats to aquatic taxa in an arid landscape:
442 Knowledge gaps and areas of understanding for amphibians of the American Southwest.
443 *WIREs Water*, 7(4), e1449. <https://doi.org/10.1002/wat2.1449>

444 Moore, C. E., Helmann, J. S., Chen, Y., St. Amour, S. M., Hallmark, M. A., Hughes, L. E., et al.
445 (2020). Anuran Traits of the United States (ATraIU): a database for anuran traits-based
446 conservation, management, and research. *Ecology*, n/a(n/a), e03261.
447 <https://doi.org/10.1002/ecy.3261>

448 Murray-Hudson, M., Wolski, P., Cassidy, L., Brown, M. T., Thito, K., Kashe, K., &
449 Mosimanyana, E. (2015). Remote sensing-derived hydroperiod as a predictor of
450 floodplain vegetation composition. *Wetlands Ecology and Management*, 23(4), 603-616.
451 <https://doi.org/10.1007/s11273-014-9340-z>

452 Ozesmi, S. L., & Bauer, M. E. (2002). Satellite remote sensing of wetlands. *Wetlands Ecology
453 and Management*, 10(5), 381-402. <https://doi.org/10.1023/A:1020908432489>

454 Parsley, M. B., Torres, M. L., Banerjee, S. M., Tobias, Z. J. C., Goldberg, C. S., Murphy, M. A.,
455 & Mims, M. C. (2020). Multiple lines of genetic inquiry reveal effects of local and
456 landscape factors on an amphibian metapopulation. *Landscape Ecology*, 35(2), 319-335.
457 <https://doi.org/10.1007/s10980-019-00948-y>

458 Paton, P. W. C., & Crouch III, W. B. (2002). Using the phenology of pond-breeding amphibians
459 to develop conservation strategies. *Conservation Biology*, 16(1), 194-204.
460 <https://doi.org/10.1046/j.1523-1739.2002.00260.x>

461 R Development Core Team. (2018). R: A language and environment for statistical computing.
462 Austria, Vienna: R Foundation for Statistical Computing. Retrieved from [http://R-](http://R-project.org)
463 [project.org](http://R-project.org)

464 Razgour, O., Korine, C., & Saltz, D. (2010). Pond characteristics as determinants of species
465 diversity and community composition in desert bats. *Animal Conservation*, 13(5), 505-
466 513. <https://doi.org/10.1111/j.1469-1795.2010.00371.x>

467 Rogers, T. N., & Chalcraft, D. R. (2008). Pond hydroperiod alters the effect of density-dependent
468 processes on larval anurans. *Canadian Journal of Fisheries and Aquatic Sciences*, 65(12),
469 2761-2768. <https://doi.org/10.1139/F08-177>

470 Ruetz III, C. R., Trexler, J. C., Jordan, F., Loftus, W. F., & Perry, S. A. (2005). Population
471 dynamics of wetland fishes: spatio-temporal patterns synchronized by hydrological
472 disturbance? *Journal of Animal Ecology*, 74(2), 322-332. [https://doi.org/10.1111/j.1365-](https://doi.org/10.1111/j.1365-2656.2005.00926.x)
473 [2656.2005.00926.x](https://doi.org/10.1111/j.1365-2656.2005.00926.x)

474 Ryan, T. J., & Winne, C. T. (2001). Effects of hydroperiod on metamorphosis in *Rana*
475 *sphenocephala*. *The American Midland Naturalist*, 145(1), 46-53, 48.
476 [https://doi.org/10.1674/0003-0031\(2001\)145\[0046:EOHOMI\]2.0.CO;2](https://doi.org/10.1674/0003-0031(2001)145[0046:EOHOMI]2.0.CO;2)

477 Schriever, T. A., Bogan, M. T., Boersma, K. S., Cañedo-Argüelles, M., Jaeger, K. L., Olden, J.
478 D., & Lytle, D. A. (2015). Hydrology shapes taxonomic and functional structure of desert
479 stream invertebrate communities. *Freshwater Science*, 34(2), 399-409.
480 <https://doi.org/10.1086/680518>

481 Schriever, T. A., & Williams, D. D. (2013). Influence of pond hydroperiod, size, and community
482 richness on food-chain length. *Freshwater Science*, 32(3), 964-975.
483 <https://doi.org/10.1899/13-008.1>

484 Sheppard, P., Comrie, A., Packin, G., Angersbach, K., & Hughes, M. (2002). The climate of the
485 US Southwest. *Climate Research*, 21, 219-238. <https://doi.org/10.3354/cr021219>

486 Skelly, D. K. (1997). Tadpole communities: pond permanence and predation are powerful forces
487 shaping the structure of tadpole communities. *American Scientist*, 85(1), 36-45.
488 www.jstor.org/stable/27856689

489 Sowder, C., & Steel, E. A. (2012). A note on the collection and cleaning of water temperature
490 data. *Water*, 4(3), 597-606. <https://doi.org/10.3390/w4030597>

491 Srikanthan, R., & McMahon, T. A. (2001). Stochastic generation of annual, monthly and daily
492 climate data: A review. *Hydrology and Earth System Sciences*, 5(4), 653-670.
493 <https://doi.org/10.5194/hess-5-653-2001>

494 Stendera, S., Adrian, R., Bonada, N., Cañedo-Argüelles, M., Hugueny, B., Januschke, K., et al.
495 (2012). Drivers and stressors of freshwater biodiversity patterns across different
496 ecosystems and scales: a review. *Hydrobiologia*, 696(1), 1-28.
497 <https://doi.org/10.1007/s10750-012-1183-0>

498 Tournier, E., Besnard, A., Tournier, V., & Cayuela, H. (2017). Manipulating waterbody
499 hydroperiod affects movement behaviour and occupancy dynamics in an amphibian.
500 *Freshwater Biology*, 62(10), 1768-1782. <https://doi.org/10.1111/fwb.12988>

501 Visser, I., & Speekenbrink, M. (2010). depmixS4: An R Package for Hidden Markov Models.
502 *Journal of Statistical Software*, 36(7), 21. <https://doi.org/10.18637/jss.v036.i07>

503 Waterkeyn, A., Grillas, P., Vanschoenwinkel, B., & Brendonck, L. (2008). Invertebrate
504 community patterns in Mediterranean temporary wetlands along hydroperiod and salinity
505 gradients. *Freshwater Biology*, 53(9), 1808-1822. <https://doi.org/10.1111/j.1365-2427.2008.02005.x>

506
507 Werner, E. E., Skelly, D. K., Relyea, R. A., & Yurewicz, K. L. (2007). Amphibian species
508 richness across environmental gradients. *Oikos*, 116(10), 1697-1712.
509 <https://doi.org/10.1111/j.0030-1299.2007.15935.x>

510